

## Geochemistry and $^{40}\text{Ar}/^{39}\text{Ar}$ age of Early Carboniferous dolerite sills in the southern Baltic Sea

Gediminas Motuza<sup>a</sup>, Saulius Šliaupa<sup>b</sup> and Martin J. Timmerman<sup>c</sup>

<sup>a</sup> Department of Geology and Mineralogy, Vilnius University, Čiurlionio 21, LT-03101, Vilnius, Lithuania; gediminas.motuza@gf.vu.lt

<sup>b</sup> Nature Research Centre, Akademijos 2, LT-08412, Vilnius, Lithuania; sliaupa@geo.lt

<sup>c</sup> Institut für Erd- und Umweltwissenschaften, Universität Potsdam, Karl-Liebknecht-Str. 24-25, D-14476 Potsdam-Golm, Germany; timmer@geo.uni-potsdam.de

Received 14 November 2014, accepted 30 January 2015

**Abstract.** The Early Carboniferous magmatic event in the southern Baltic Sea is manifested by dolerite intrusions. The presumable area in which the dolerite intrusions occur ranges from 30 to 60 km in east–west direction, and is about 100 km in north–south direction. The dolerites were sampled in well D1-1 and investigated by applying chemical analysis and  $^{40}\text{Ar}/^{39}\text{Ar}$  step-heating dating. Dolerites are classified as alkali and sodic, characterized by high  $\text{TiO}_2$  (3.92, 3.99 wt%) and  $\text{P}_2\text{O}_5$  (1.67, 1.77 wt%) and low  $\text{MgO}$  (4.89, 4.91 wt%) concentrations, enriched in light rare earth elements, originated from an enriched mantle magma source and emplaced in a continental rift tectonic setting. The  $351 \pm 11$  Ma  $^{40}\text{Ar}/^{39}\text{Ar}$  plateau age for groundmass plagioclase indicates a considerable age gap with the 310–250 Ma magmatism in southern Scandinavia and northern Germany. The magmatic rocks in the Baltic Sedimentary Basin are coeval with alkaline intrusions of NE Poland. Both magmatic provinces lie in the northwestward prolongation of the Pripyat–Dnieper–Donetsk Rift (370–359 Ma) and may constitute a later phase of magmatic activity of this propagating rift system.

**Key words:** dolerite, rifting, Carboniferous, argon dating, Baltic Sea.

### INTRODUCTION

The southern Baltic Sea is underlain by the Baltic Sedimentary Basin that was initiated in the late Ediacaran–Early Cambrian by the extension of a basement of predominantly Palaeoproterozoic (1.8–1.9 Ga) crystalline rocks of the East European Craton margin (Šliaupa & Hoth 2011). Major subsidence and deposition of marine sediments took place during the Late Ordovician–Middle Silurian, which was followed by SE-directed compression related to the Caledonian orogeny in the Late Silurian–Early Devonian. In this period, major E–W- and NE–SW-striking faults were formed in the basin and partial erosion took place. Sedimentation resumed with the deposition of Devonian shallow-marine and terrestrial sediments and, locally, of thin Lower Carboniferous sandstones and shales, and was followed by a break until the mid–late Permian. The deposition in the Late Permian, Mesozoic and Cenozoic was mostly of terrestrial nature, punctuated by marine incursions, and is characterized by long periods of non-deposition. Total thicknesses of sediments vary from 2300 m in western Lithuania to over 4000 m in the western part of the basin. No volcanic or intrusive magmatic rocks are known from the Baltic Sedimentary Basin.

The occurrence of dolerite intrusions in the southern Baltic Sea was first reported in the 1980s after the drilling of two offshore oil exploration wells, D1-1 and C8-1 (Fig. 1) (Motuza et al. 1994). The wells were drilled in the first place because the seismic velocity data had been misinterpreted. As the presence of dolerite intrusions in the Baltic Sea area was not known previously, no correction for the seismic pull-up effect due to the high seismic velocity of dolerite had been applied during seismic data processing, which caused an incorrect definition of the prospective uplifts in the underlying oil-bearing Middle Cambrian reservoir. The seismic data were re-interpreted after drilling the wells, and it was realized that the presence of the so-called seismic disrupted ‘Y’ reflector in the Silurian succession was related to dolerite bodies that, based on the seismic data, were interpreted as sills (unpublished industrial reports).

Based on industrial seismic data the size of the presumable area in which dolerite intrusions occur ranges from 30 to 60 km in east–west direction, and is about 100 km in north–south direction (Fig. 1). Dolerites were discovered in wells D1-1 and C8-1 by drilling the lower part of Upper Silurian shales at depths of 1698–1722 m and 1977–1983 m, respectively (Fig. 2)

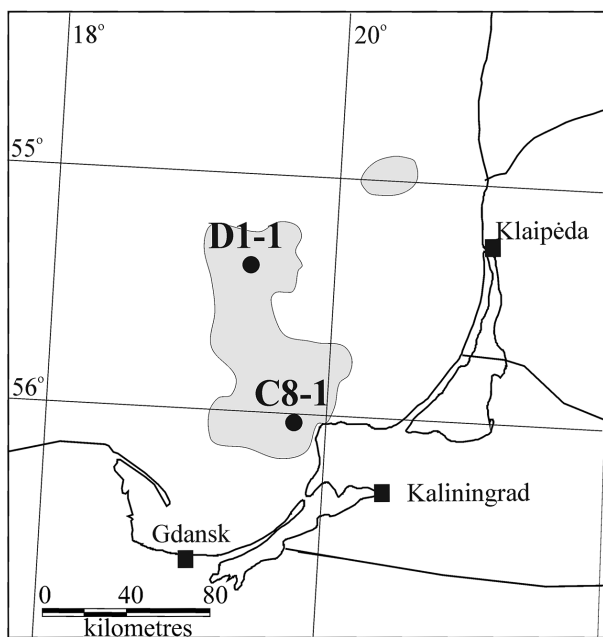


**Fig. 1.** Distribution of dolerite sills defined by seismic (shaded areas) and drilling (black dots) data.

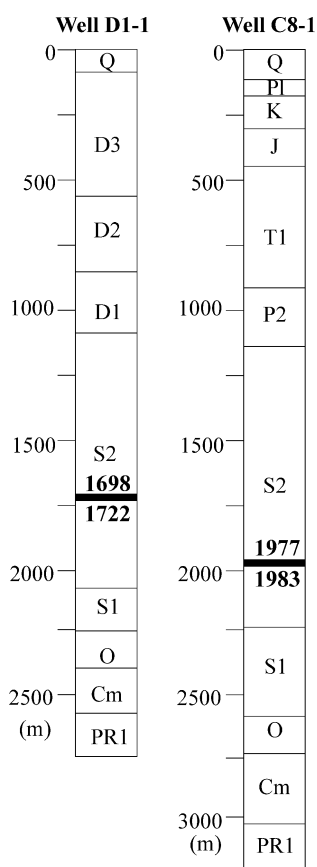


**Fig. 2.** Geological sections of wells D1-1 and C8-1 (see Fig. 1 for locations). Dolerite sills are marked by a thick line.

(unpublished industrial reports). The industrial seismic data also indicate the presence of a second, smaller (ca 20 km × 20 km) igneous field in the northern part of the Lithuanian and adjacent Latvian offshore.

Previous K–Ar whole-rock dating yielded ages in the range 310–370 Ma (Šliaupa et al. 2002) suggesting Palaeozoic intrusion ages. However, these ages are too imprecise to allow the assignment of the Baltic sills to one of the main magmatic events in the larger region: late Devonian (e.g. Pripyat–Dnieper–Donetsk Rift), early Carboniferous (central and NE Poland) or late Carboniferous–early Permian (SE Scandinavia) events. In order to better position the isolated occurrence of the Baltic dolerite sills in the geological evolution of the region, we used the obtained new  $^{40}\text{Ar}/^{39}\text{Ar}$  dating results of a whole-rock and a groundmass plagioclase sample in combination with whole-rock major and trace element data.

## ANALYTICAL METHODS

### Chemical analysis

The chemical composition of dolerite was determined from two whole-rock samples D1-1 and D1-2, each of the two main varieties characterized below. Geochemical analyses were conducted at Acme Analytical Laboratories Ltd., Vancouver, Canada, using the ICP-AES and ICP-MS techniques.

### $^{40}\text{Ar}/^{39}\text{Ar}$ step-heating dating

Dolerite sample D1-1 was crushed in a jaw breaker and sieved into grain size fractions. The 170–250 µm groundmass plagioclase size fraction was obtained by repeated passes through a Frantz magnetic separator at increasing field strengths. Both groundmass plagioclase and the 170–250 µm whole-rock grain size fraction were leached in an ultra-sonic bath for 10 min in ca 1 M  $\text{HNO}_3$  to remove any carbonates present. It was followed by rinsing the samples in de-ionized water, and leaching for ca 10 min in 7% HF to break down alteration products. The whole-rock sample was cleaned in de-ionized water for 10 min and handpicked under an overview microscope (40 times magnification) to remove any altered grains. The groundmass plagioclase was leached following the same procedure and subsequently sieved again and further concentrated using a Frantz magnetic separator. The final plagioclase separate was cleaned and purified by handpicking under an overview microscope against a dark background (to remove grains showing signs of alteration showing up as white patches) and a light background (to remove grains with inclusions).

The  $^{40}\text{Ar}/^{39}\text{Ar}$  analysis of whole-rock sample D1-1 was performed at Leeds University using a modified, semi-automatic AEI MS10 mass spectrometer. Gas extraction was carried out by stepwise heating in a double-vacuum resistance heated furnace. Sample temperature was measured using an infrared optical pyrometer and is estimated to be accurate to  $\pm 25^\circ\text{C}$ . For run 2483 ca 50 mg of material was irradiated in high-purity Al foil at the Risø reactor in Roskilde (Denmark) for 10 h. The interference correction factors are listed with the analytical data in Table 1. The neutron flux variation over the length of the canister was monitored by co-irradiated biotite standards Tinto (409.2 Ma, Rex & Guise 1986) and LP-6 (Engells & Ingamels 1971; Roddick 1983) and was of the order of 3%. The Tinto standard was cross calibrated against HB3gr (Turner et al. 1971), Fy12a (Roddick 1983) and MMHb-1 (Alexander et al. 1978); the ages used for each of these standards are as given in Roddick (1983). The analytical data for the whole-rock sample were collected and processed at Leeds University using the in-house developed software (see Rex et al. 1993) and plotted using ‘Isoplot for Excel’ by Ludwig (1998).

The  $^{40}\text{Ar}/^{39}\text{Ar}$  analysis of groundmass plagioclase sample D1-1 was carried out at the Vrije Universiteit (VU) in Amsterdam using the VULKAAN  $^{40}\text{Ar}/^{39}\text{Ar}$  CO<sub>2</sub> laser probe and a MAP 215-50 double focusing noble gas mass spectrometer fitted with a Johnston MM1 secondary electron multiplier detector (Wijbrans et al. 1995). The plagioclase separate (ca 78 mg) was wrapped in Al foil, loaded together with other samples and standards in cylindrical Al containers (position C23)

and irradiated as batch VU-36 at the Triga CLICIT Reactor facility at Oregon State University for 12 h together with the flux monitor DRA (Drachenfels sanidine) of age 25.26 Ma (Wijbrans et al. 1995; Renne et al. 1997). The interference correction factors for run number 01M0008 are listed together with the analytical data in Table 2. The sample was loaded in 8 mm diameter and 3 mm deep copper sample pans. Stepwise heating was done with a defocussed laser beam and the ‘ArArCalc’ software was used for online data acquisition and data reduction (Koppers 2002). Before analysis the sample was heated with a 0.3 W defocussed beam to remove adsorbed atmospheric gases. Further information on the analytical techniques at the Vrije Universiteit can be found in Wijbrans et al. (1995) and Kalt et al. (2000).

All ages were calculated using the decay constants and  $^{40}\text{K}$  abundance recommended by Steiger & Jäger (1977).

### Sample description

The total thickness of the dolerite body penetrated and cored by well D1-1 was estimated by well-logging at ca 25 m; the core was collected from the 5.5 m thick uppermost part of the sill (interval 1698–1703.5 m). Thin sections of the dolerite were examined and two petrographic types were recognized in the cored interval: a fine-grained type and a very fine-grained type. Both rock types alternate in the interval whereby the fine-grained dolerite predominates. It is brecciated at the contacts, suggesting a younger age for the very fine-grained variety and indicating that sill emplacement

**Table 1.**  $^{40}\text{Ar}/^{39}\text{Ar}$  data of step-heating dating of leached whole-rock dolerite sample D1-1 1/84 (MS10, Leeds University, Leeds run number 2483). Errors quoted on 1-sigma level.  $^{*40}\text{Ar}$  = volume of radiogenic  $^{40}\text{Ar}$ , gas volumes corrected to standard temperature and pressure. Sample grain size 170–250  $\mu\text{m}$ , sample weight = 0.05302 g, K = 1.2 wt%. No plateau age could be calculated; total gas age =  $335.0 \pm 1.6$  Ma. The error on the total gas age includes the uncertainty in the irradiation parameter ( $J$ ), but the individual steps are reported with analytical errors only. Ages were calculated using the constants recommended by Steiger & Jäger (1977). The interference correction factors were  $(^{40}\text{Ar}/^{39}\text{Ar})_{\text{K}} = 0.048$ ,  $(^{36}\text{Ar}/^{39}\text{Ar})_{\text{Ca}} = 0.038$  and  $(^{37}\text{Ar}/^{39}\text{Ar})_{\text{Ca}} = 1492$ .  $^{*40}\text{Ar} = 173 \times 10^{-7} \text{ cm}^3 \text{ g}^{-1}$ ,  $J$  value =  $0.00550 \pm 0.5\%$

Temperature (°C)	$^{39}\text{Ar}_{\text{K}}$	$^{37}\text{Ar}_{\text{Ca}}$	$^{38}\text{Ar}_{\text{Cl}}$	Ca/K	$^{*40}\text{Ar}/^{39}\text{Ar}_{\text{K}}$	$^{40}\text{Ar}_{\text{atm}}$ (%)	Age (Ma)	Error (Ma)	$^{39}\text{Ar}_{\text{K}}$ (%)
	Vol. $\times 10^{-9} \text{ cm}^3$								
546	0.5	0.9	0.1	3.3	13.80	93.5	132.0	7.4	2.1
690	1.6	4.2	0.2	5.3	37.15	48.6	335.4	1.7	6.5
760	1.8	2.2	0.5	2.4	38.49	15.9	346.4	1.3	7.4
850	4.8	3.8	1.5	1.6	38.80	4.3	348.9	0.7	19.6
914	4.3	2.7	1.5	1.3	38.50	1.4	346.5	0.6	17.3
976	3.3	2.8	1.0	1.7	37.65	1.2	339.6	1.0	13.3
1025	1.8	3.0	0.4	3.3	37.25	0.6	336.2	1.6	7.3
1103	3.1	11.6	0.7	7.5	35.96	3.1	325.5	0.6	12.4
1190	2.7	17.0	0.5	12.3	35.87	5.9	324.9	0.6	11.1
1296	0.8	6.8	0.1	18.0	37.33	21.2	336.9	3.5	3.1

**Table 2.**  $^{40}\text{Ar}/^{39}\text{Ar}$  data of step-heating dating of groundmass plagioclase from dolerite sample D1-1 1/84 (Vrije Universiteit, Amsterdam; run 01M0008). Errors quoted on 2-sigma level.  $^{40}\text{Ar}_{\text{corr}}$  = corrected atmospheric  $^{40}\text{Ar}$ . Sample grain size 170–250  $\mu\text{m}$ , sample weight = 78 mg. Plateau age =  $351 \pm 11$  Ma (all steps); normal isotope correlation age =  $349 \pm 74$  Ma, inverse isotope correlation age =  $345 \pm 12$  Ma. Errors on ages include the uncertainty in the irradiation parameter ( $J$ ), but the individual steps are reported with analytical errors only. Ages were calculated using the constants recommended by Steiger & Jäger (1977). The interference correction factors were  $(^{36}\text{Ar}/^{37}\text{Ar})_{\text{Ca}} = 0.000264$ ,  $(^{39}\text{Ar}/^{37}\text{Ar})_{\text{Ca}} = 0.000673$ ,  $(^{40}\text{Ar}/^{39}\text{Ar})_{\text{K}} = 0.00086$ .  $J$  value = 0.003093; mass discrimination value = 0.995

Laser output (W)	$^{36}\text{Ar}_{\text{atm}}$	$^{37}\text{Ar}_{\text{Ca}}$	$^{38}\text{Ar}_{\text{Cl}}$	$^{39}\text{Ar}_{\text{K}}$	$^{40}\text{Ar}_{\text{corr}}$ (%)	Age (Ma)	$\pm 2$ -sigma (Ma)	$^{39}\text{Ar}_{\text{K}}$ (%)	Ca/K
0.60	0.00700	0.23688	0.00000	0.02491	44.8	340.8	97.1	2.5	22.1
0.80	0.00361	0.00000	0.00000	0.03799	71.4	353.7	59.3	3.8	449.9
1.10	0.00343	0.48558	0.00004	0.08205	84.6	343.7	31.7	8.1	13.8
1.30	0.00089	0.55969	0.00000	0.06048	94.2	358.5	46.3	6.03	21.5
1.60	0.00111	0.55905	0.00000	0.07017	93.6	345.5	32.9	7.0	18.5
2.05	0.00031	0.00000	0.00000	0.01454	91.1	327.9	204.1	1.4	611.7
3.00	0.00043	0.30258	0.00000	0.04907	96.3	345.2	56.4	4.9	14.3
4.00	0.00056	0.31315	0.00173	0.04754	95.1	338.1	56.4	4.7	15.3
5.50	0.00044	1.02718	0.00136	0.09234	98.0	347.4	28.2	9.2	25.9
7.50	0.00000	0.90618	0.00107	0.06550	100.0	357.8	10.3	6.5	32.2
9.00	0.00039	1.12189	0.00014	0.10789	98.5	347.3	23.4	10.7	24.2
12.00	0.00087	1.18878	0.00000	0.11957	96.9	345.0	19.4	11.9	23.1
22.00	0.00196	2.36067	0.00000	0.23348	96.5	347.5	11.3	23.2	23.5

took place in at least two stages. The fine-grained variety was sampled in the interval 1700.6–1703.5 m (sample D1-1) and the very fine-grained in the interval 1699.1–1700.6 m (sample D1-2).

The fine-grained dolerite is characterized by a porphyritic texture (Fig. 3A). The matrix has a poikilophitic texture formed predominantly by plagioclase (labradorite,

$\text{An}_{60-65}$ , in some grains bytownite,  $\text{An}_{70-75}$ ) enclosed by elongated hypidiomorphic brownish augite crystals of 0.3–0.8 mm length and isometric grains of subordinated olivine and biotite; accessory phases are apatite and magnetite. The plagioclase phenocrysts ( $\text{An}_{60-65}$ ) are euhedral, a few millimetres long with weakly zoned marginal parts. They comprise 5% of the rock volume.

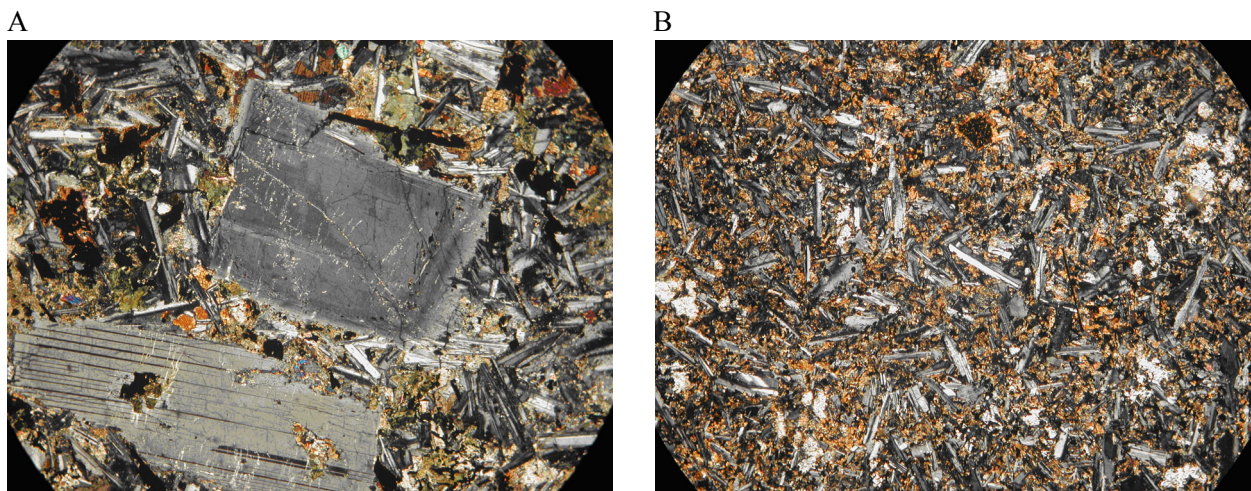


**Fig. 3.** Microphotograph of the dolerite from well D1-1: **A**, fine-grained; **B**, very fine-grained. The base of the picture is 4.5 mm long.

Very fine-grained dolerite sample D1-2 is also porphyritic. The predominant size of the crystals making up the groundmass is in the range 0.1–0.3 mm. It is predominantly composed of plagioclase (labradorite, An<sub>60–65</sub>) (Fig. 3B). Biotite, actinolite, chlorite and talc formed at the expense of primary olivine and pyroxene that are not preserved. The plagioclase phenocrysts (bytownite, An<sub>75</sub>) are idiomorphic, slightly zoned of 3–4 mm length, comprising around 3% of the rock volume.

## RESULTS

### <sup>40</sup>Ar/<sup>39</sup>Ar dating

#### Whole-rock sample

<sup>40</sup>Ar/<sup>39</sup>Ar step-heating analysis of whole-rock sample D1-1 did not result in a plateau age. Figure 4A shows the convex gas release spectrum in which the apparent ages increase from ca 335 Ma for heating step 2 to ca 349 Ma for step 4. Subsequently the apparent ages decrease to ca 325 Ma for steps 8 and 9. Calculating a weighted-mean age for the gas fractions of steps 3–5

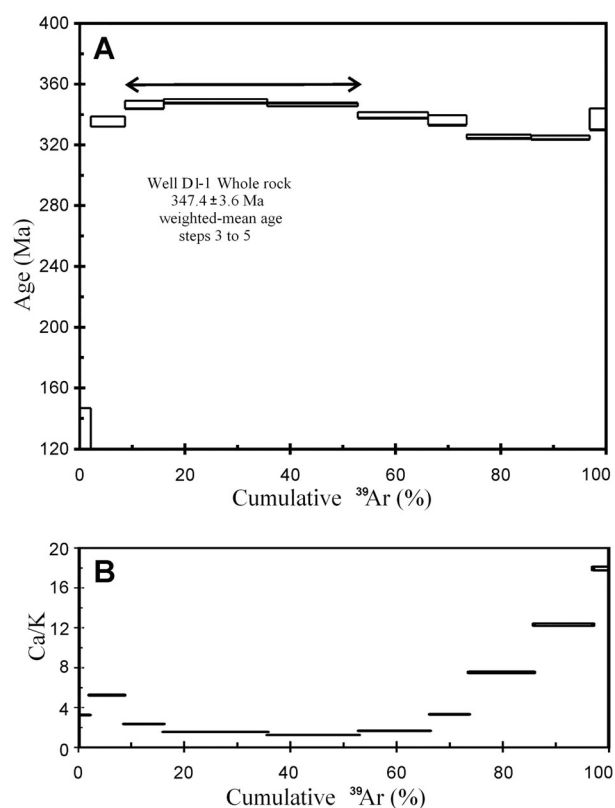


**Fig. 4.** A, gas release spectrum for whole-rock sample D1-1 (Leeds run 2483). Steps 3–5 yield a ca  $347 \pm 3.6$  Ma weighted-mean age. B, Ca/K vs released <sup>39</sup>Ar diagram showing a concave pattern.

(Fig. 4A) yields an age of  $347 \pm 3.6$  Ma (mean square of weighted deviates (MSWD) = 4.3), comprising only 44% of the <sup>39</sup>Ar released. The total gas age is  $335 \pm 1.6$  Ma (Table 1). Due to excess scatter and absence of a plateau, no isotope correlation age can be calculated. The Ca/K vs released <sup>39</sup>Ar diagram (Fig. 4B) shows that Ca/K increases with increasing temperature; this is likely to be due to breakdown and degassing of a phase with high Ca/K.

#### Groundmass plagioclase

<sup>40</sup>Ar/<sup>39</sup>Ar step-heating analysis of the groundmass plagioclase fraction of sample D1-1 resulted in a  $351 \pm 11$  Ma weighted-mean age for all 13 steps (MSWD = 0.29), which can be interpreted as a plateau age at 2-sigma level (Fig. 5A, Table 2) and the time of dolerite crystallization. The large age uncertainty is the result of elevated background levels due to an unfortunate atmospheric leak that had occurred in the week before analysis. The plateau age is supported by the similar  $349 \pm 74$  Ma normal (Fig. 5B) and  $345 \pm 12$  inverse isotope correlation ages (Fig. 5C). The <sup>40</sup>Ar/<sup>36</sup>Ar intercept values are, respectively,  $291.0 \pm 106.2$  and  $295.3 \pm 66.0$  (both 2-sigma), rather imprecise but overlapping the accepted value for air (295.5), suggesting that excess argon was not present. The Ca/K ratios do not show large variations, suggesting that the plagioclase fraction was relatively pure (Table 2; Fig. 5B). Despite the relative large analytical uncertainties, the data clearly show that the sill intruded and crystallized in Early Carboniferous times.

## Geochemistry

The major and trace element compositions of two whole-rock samples were determined, one of each dolerite variety (Table 3). The compositions of both dolerite varieties were found to be quite similar. On the total alkali vs silica (TAS) diagram, both analyses cluster in the tephrite–basanite field on the border with the basalt field, while in the Nb/Y vs Zr/TiO<sub>2</sub> diagram they plot in the alkali basalt field (Fig. 6). The K<sub>2</sub>O/Na<sub>2</sub>O ratios of 0.50 and 0.53 indicate that the rocks are sodic rather than potassic. They are furthermore characterized by very high TiO<sub>2</sub> (3.92 and 3.99 wt%) and P<sub>2</sub>O<sub>5</sub> (1.67 and 1.77 wt%) concentrations and low MgO (4.89 and 4.91 wt%), Ni (26 and 28 ppm) and Cr (4 and 5 ppm) contents. The low MgO contents and Sr troughs on the multi-element diagram (Fig. 7) indicate fractional crystallization of mafic minerals and early fractionation of plagioclase, the latter being in agreement with the presence of plagioclase phenocrysts.

The dolerite is enriched in light rare earth elements (LREEs) compared to chondrite: the La<sub>N</sub> (chondrite-normalized) values are 145 and 148, the (La/Yb)<sub>N</sub> ratios

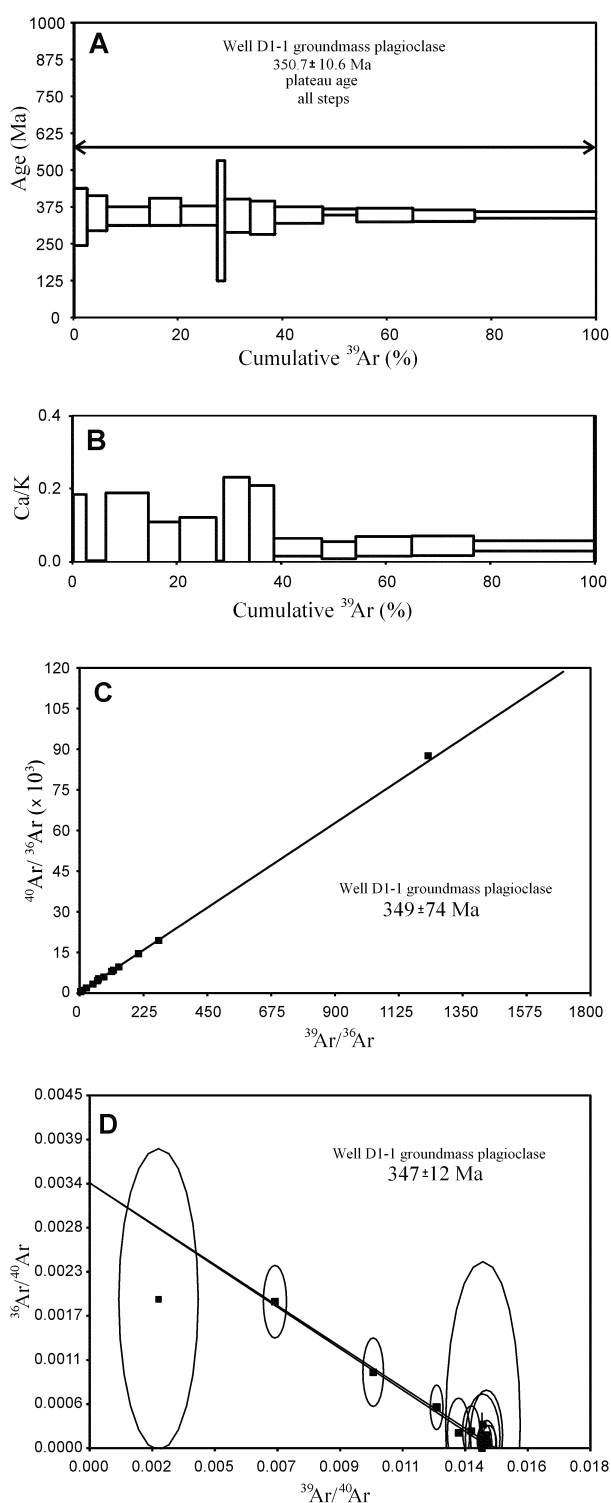


**Fig. 5.** **A**, gas release spectrum for groundmass plagioclase from sample D1-1 (VU run 01M0008). The weighted mean age for all 13 steps is  $351 \pm 11$  Ma (2-sigma). **B**, Ca/K vs released  $^{39}\text{Ar}$  diagram showing a constant Ca/K ratio. **C**,  $349 \pm 74$  Ma normal isotope correlation age. **D**,  $347 \pm 12$  Ma inverse isotope correlation age.

are, respectively, 13.9 and 14.1 (Fig. 7A), indicating a relatively high degree of LREE enrichment, whereas the Yb concentrations are 10 times those of chondrite (Fig. 7A). The samples also have elevated amounts of incompatible elements with respect to primitive mantle- and normal-type mid-ocean ridge basalt (N-MORB), but have comparatively lower amounts of Th, U, Sr and Zr (Fig. 7B, C). The multi-element patterns of dolerites show the closest fit with those of ocean island basalts (OIB) (Fig. 7D).

On tectonic setting discrimination diagrams the samples plot within the continental rift basalt fields (Fig. 8). High Th/Yb (1.1, 1.1) and Ta/Yb (0.8, 0.9) ratios show the affinity of the dolerites to within-plate alkali basalts and indicate an enriched mantle as a possible magma source (Fig. 9), and so do the low Zr/Nb ratios ( $\sim 5$ ) (Sun & McDonough 1989). The  $\Delta\text{Nb}$  parameter ( $= \log(\text{Nb}/\text{Y}) + 1.74 - 1.92 \times \log(\text{Zr}/\text{Y})$ ) of Fitton et al. (1997) is high (0.4, 0.4) and supports a mantle source. Low Nb/La ratios (0.7, 0.7) point to asthenosphere-derived magmas mixed with some lithospheric mantle (McDonough et al. 1992) and the Nb/U ratios of ca 50 are characteristic of basalts uncontaminated by crustal material (Hofmann et al. 1986).

## DISCUSSION

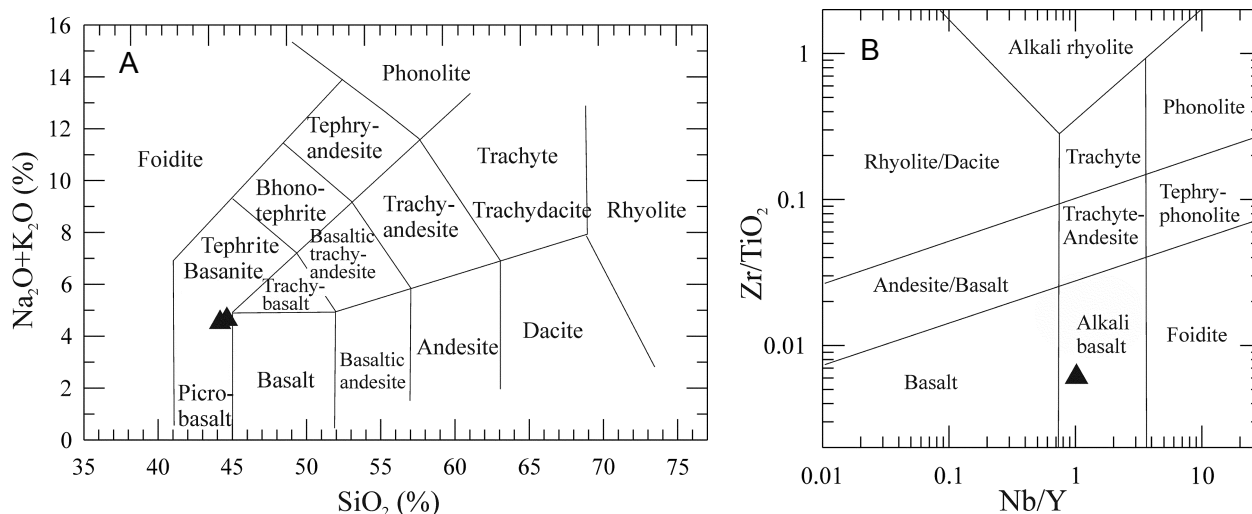
### Regional correlation

Late Palaeozoic intrusive and volcanic rocks are widespread north of the Variscan orogen and constitute an early Carboniferous–early Permian igneous province that extends from SW Ireland over Scotland, southern Scandinavia, to the North German Basin and adjacent areas. Magmatic activity occurred within the time span of ca 350–250 Ma but was intermittent, of varying composition and triggered by different tectonic events and mechanisms (Timmerman 2004, and references therein). Magmatism in southern Norway (Oslo Rift), southern Sweden, northern Germany and western Poland was limited to the period 310–250 Ma (Breitkreuz & Kennedy 1999; Neumann et al. 2004; Timmerman et al. 2009). The early Carboniferous  $^{40}\text{Ar}/^{39}\text{Ar}$  age of sample D1-1 clearly shows that the Baltic dolerite sills do not belong to this magmatic stage.

The nearest magmatic rocks of similar age are alkaline intrusions in northeastern Poland, ca 150–300 km to the south and southeast (Fig. 10). Here, three magmatic massifs (Ełk, Pisz and Tajno) were identified by drilling through the Mesozoic–Cenozoic cover into the crystalline basement of the East European Craton, or their presence was inferred from preliminary data in the Mława and Olsztynek areas. Except for the Mława area intrusion, the plutons form an east–west-trending chain (Fig. 10).

**Table 3.** Chemical composition of dolerites, well D1-1 (major elements in %, trace elements in ppm)

Element	Sample D1-1	Sample D1-2	Element	Sample D1-1	Sample D1-2
SiO <sub>2</sub>	44.22	44.77	Sm	10.56	10.94
Al <sub>2</sub> O <sub>3</sub>	14.32	14.52	Eu	4.07	4.25
Fe <sub>2</sub> O <sub>tot</sub>	14.92	14.71	Gd	9.19	9.58
MgO	4.91	4.86	Tb	1.22	1.25
CaO	8.59	8.33	Dy	6.48	6.55
Na <sub>2</sub> O	3.02	3.13	Ho	1.05	1.10
K <sub>2</sub> O	1.60	1.55	Er	2.69	2.77
TiO <sub>2</sub>	3.92	3.99	Tm	0.37	0.37
P <sub>2</sub> O <sub>5</sub>	1.67	1.77	Yb	2.15	2.23
MnO	0.21	0.20	Lu	0.30	0.30
LOI	2.2	1.7	Mo	1.0	0.7
Ni	21.0	43.0	Cu	35.0	30.8
Sc	21.0	22.0	Pb	3.3	8.7
Ba	1537.0	1576.0	Zn	90.0	124.0
Be	1.0	<1.0	Ni	26.2	28.7
Co	40.7	41.9	Au	1.7	<0.5
Cs	0.8	0.8	Co	32.0	33.5
Ga	21.4	21.6	Mn	817.0	709.0
Hf	3.7	3.5	As	0.9	0.5
Nb	29.5	30.6	U	0.3	0.4
Rb	26.6	24.2	Th	1.4	1.5
Sr	815.0	836.0	Sr	182.0	192.0
Ta	1.8	1.9	Cd	<0.1	0.3
Th	2.3	2.6	V	90.0	103.0
U	0.6	0.6	La	40.0	45.0
V	288.0	295.0	Cr	4.0	5.0
Zr	156.1	159.1	Ba	232.0	289.0
Y	30.6	31.2	Hg	0.02	<0.01
La	44.9	45.9	Sc	3.1	3.6
Ce	96.9	100.1	Tl	0.1	0.1
Pr	12.65	13.20	Ga	8.0	9.0
Nd	54.7	56.0	Se	1.7	1.0

**Fig. 6.** Classification diagrams for dolerite from well D1-1: **A**, total alkali vs silica; **B**, Zr/TiO<sub>2</sub> vs Nb/Y of Winchester & Floyd (1977).

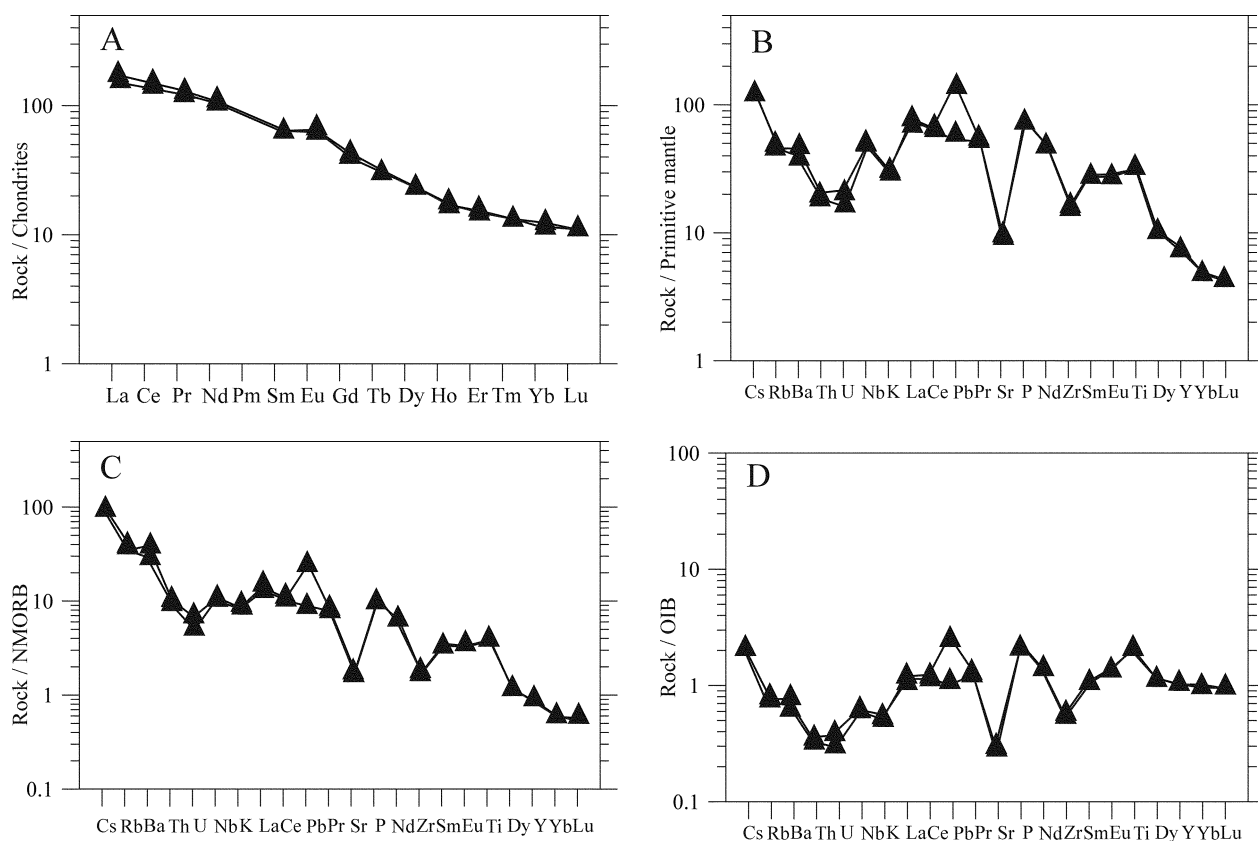


**Fig. 7.** Abundance of rare earth elements and multi-element diagrams for dolerite from well D1-1. Abbreviations: N-MORB, normal-type mid-ocean ridge basalt; OIB, ocean island basalt.

The Tajno massif is composed of alkaline rocks ranging from syenite to pyroxenite, cut by carbonatite veins (Krystkiewicz & Krzemiński 1992; Ryka 1992; Ryka et al. 1992). The composite Elk massif was formed during several stages of igneous activity and consists predominantly of syenites, feldspathoid-bearing syenites and foidolites (Dziedzic & Ryka 1983; Armbrustmacher & Modreski 1994). The composition of the Pisz intrusion is poorly known as only a single drill hole has been drilled into it, yielding alkaline gabbro (gabbro–syenite). In addition, syenites cutting basement rocks and Palaeozoic sediments were identified in four wells around the Mława geophysical anomaly (Krzemińska & Krzemiński 2012).

The U–Pb SIMS and SHRIMP zircon ages for the Pisz and Elk intrusions yielded crystallization ages of  $345.5 \pm 5.1$  and  $347.7 \pm 7.9$  Ma, respectively. Intercept ages of  $254 \pm 9$  to  $348 \pm 15$  Ma were obtained for Tajno syenites. Pyrrhotite from a Tajno carbonatite vein, dated by the Re–Os method, yielded an age of 348 Ma (Demaiffe et al. 2013). These ages agree with previously obtained  $347.7 \pm 8$  and  $345.5 \pm 5$  Ma U–Pb zircon ages for, respectively, the Elk and Pisz intrusions (Krzemińska

et al. 2006; Krzemińska & Krzemiński 2012). Recently, a U–Pb zircon age of  $349.1 \pm 5.7$  Ma was reported for a few decimetres thick granite vein in the Telšiai shear zone of the Proterozoic basement of West Lithuania (well Girkaliai-2, Grk in Fig. 10), 3 km to the east of the Baltic Sea (Vejeļyte et al. 2011). The 354–345 Ma published ages illustrate that plutons of alkaline and often silica undersaturated composition in NE Poland intruded coevally with the ca 351 Ma alkaline dolerite sills in the Baltic Sedimentary Basin.

In a larger-scale context, the Baltic dolerites and the alkaline rocks of northeastern Poland were preceded by magmatic activity in the Pripyat palaeorift in southern Belarus which represents the northwestern continuation of the Dnieper–Donetsk Aulacogen in Ukraine. The Pripyat Rift contains late Devonian volcanic and intrusive rocks, including high-alkali varieties (Korzun & Makhnach 1977; Petrova et al. 1983). Locally, ultramafic rocks, lamprophyre diatremes and carbonatites are present (Veretennikov et al. 1997), indirectly dated as Upper Devonian by palaeontological data from the host rocks (Kruczek & Obukhovskaya 1997). In addition, abundant basalt and dolerite sills and dykes are reported from

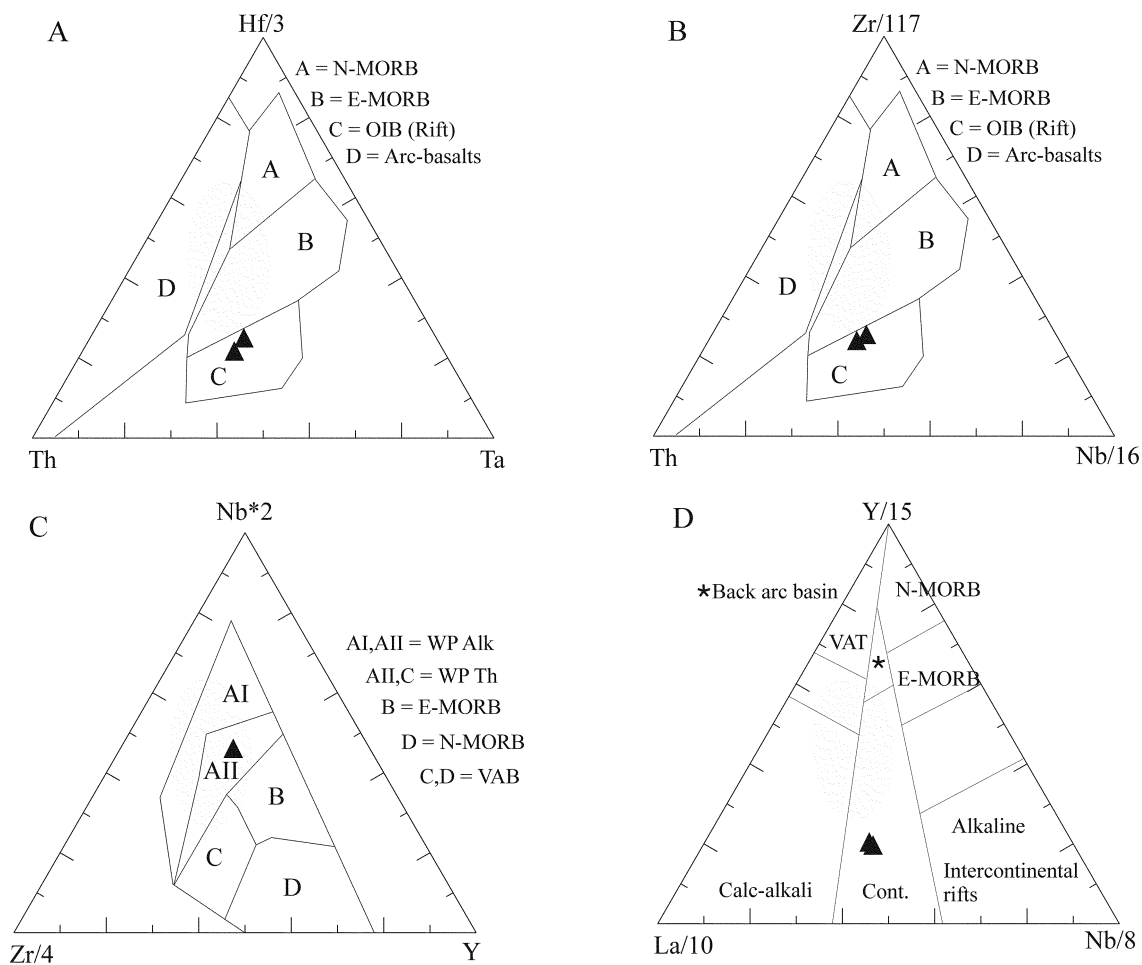


**Fig. 8.** Tectonic setting diagrams for dolerites from well D1-1: **A**, Th-Hf/3-Ta; **B**, Th-Zr/117-Nb/16 (Wood 1980); **C**, Zr/4-Nb $\times$ 2-Y (Meschede 1986); **D**, La/10-Y/15-Nb/8 (Cabanis & Lecolle 1989). E-MORB, enriched mid-ocean ridge basalt; OIB, ocean island basalt; VAB, volcanic arc basalt; VAT, volcanic arc tholeiitic basalt; WP Alk and WP Th, within plate basalt – alkaline and tholeiitic, respectively.

deep wells (Aizberg et al. 2001). The igneous activity in the Pripyat rift terminated after the extrusion of nepheline leucitites which are intercalated with Upper Frasnian–Upper Famennian sediments (370–359 Ma; Kuszniir et al. 1996). Their stratigraphic ages agree with the ca 370 Ma radiometric ages (Wilson & Lyashkevich 1996). The Sr–Nd isotope studies indicate that the parent magmas were predominantly formed by the melting of the primitive mantle, whereas some were derived from an enriched mantle source (Mikhailov et al. 2010).

In terms of composition and age, the intrusions in NE Poland and the sills in the Baltic Sedimentary Basin fit the early Carboniferous magmatic activity in the northern Variscan foreland west of the Teisseyre–Tornquist Zone (TTZ; mainly Great Britain and Ireland). Most of this can be related to small-degree mantle melting, triggered by repeated extensional reactivation

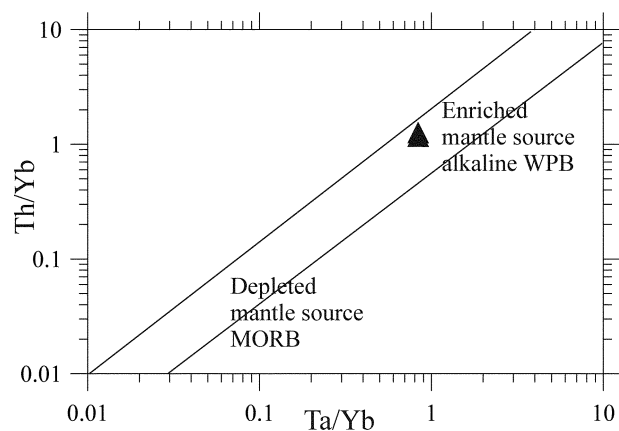


**Fig. 9.** Ta/Yb vs Th/Yb diagram for the dolerites from well D-1 (Pearce 1983, 1996). WPB, within plate basalt; MORB, middle ocean ridge basalt.

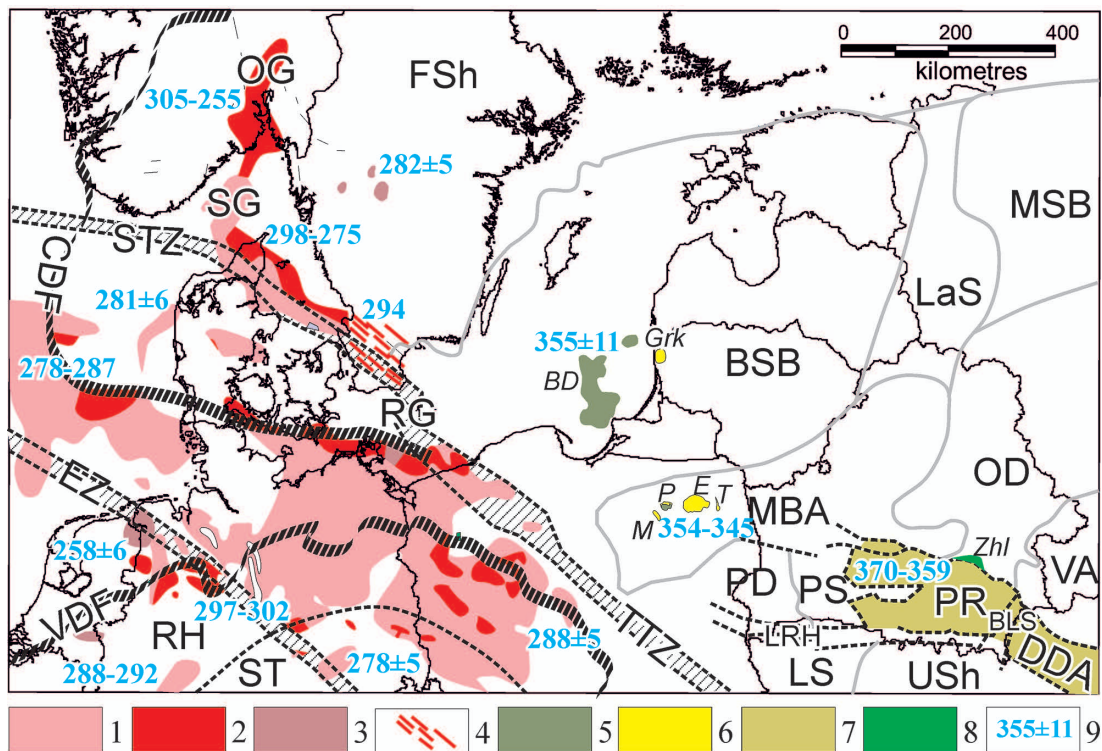


**Fig. 10.** Distribution of Permo-Carboniferous igneous rocks. Late Carboniferous–Permian igneous rocks: 1, extrusions, 2, intrusions, 3, sills, 4, dolerite dykes; Early Carboniferous igneous rocks: 5, sills (*BD*, Baltic dolerites), 6, intrusions (*E*, Elk syenite, *Grk*, Girkaliai granite, *M*, Mława syenite, *P*, Pisz gabro, *T*, Tajno carbonatites); Late Devonian igneous rocks: 7, volcanic rocks; 8, ultramafic intrusions (*Zhl*, Zhlobin); 9, age of igneous rocks (Ma). Compiled after Aizberg et al. 2001; Heeremans et al. 2004; Neumann et al. 2004; Krzemińska & Krzemiński 2012; Demaiffe et al. 2013.

Major tectonic structures: BSB, Baltic Sedimentary Basin; BLS, Bragov–Loev Saddle; CDF, Caledonian Deformation Front; DDA, Dnieper–Donetsk Aulacogen; EZ, Elba Zone; FSh, Fennoscandian Shield; LRH, Lukau–Ratno Horst; LaS, Latvian Saddle; LS, Lublin Slope; MBA, Mazury–Belarus High; MSB, Moscow Sedimentary Basin; OD, Orsha Depression; OG, Oslo Graben; PD, Podlasie Depression; PR, Pripyat Rift; PS, Polessian Saddle; RG, Rønne Graben; RH, Rhenohercynian Zone; SG, Skagerrak Graben; ST, Saxoturingian Zone; STZ, Sorgenfrei–Tornquist Zone; TTZ, Teisseyre–Tornquist Zone; USh, Ukrainian Shield; VA, Voronezh Arch; VDF, Variscan Deformation Front.

of pre-existing, deep-seated faults (e.g. Leeder 1982; Narkiewicz 2007). On the other hand, a relation with the late Devonian magmatism in the Dnieper–Donetsk Rift cannot be ruled out. Magmatic activity in the Dnieper–Donetsk Rift, NE Poland and the Baltic Sedimentary Basin entirely took place east of the TTZ in an old Precambrian crust of the East European Craton and was predominantly alkaline in composition. Narkiewicz (2007) pointed out a similar late Devonian tectono-sedimentary development of the Lublin Basin and the Pripyat–Dnieper–Donetsk Rift. Although the Lublin Basin lacks extensive syn-rift volcanism of late Devonian age, both rifts contain volcanic rocks of early Carboniferous (Viséan) age. The early Carboniferous magmatism in NE Poland and the Baltic Sedimentary Basin may reflect the latest stage of magmatic activity in a (north-) westwards migrating rift system (Narkiewicz 2007

and references therein; Demaiffe et al. 2013; Kharin & Eroshenko 2014).

### Structural setting of the Baltic sills

The dolerite field is confined to the deepest (Gdansk) basin of the present Baltic Sea and not related to areas of increased faulting. Moreover, the areas with the greatest fault density in the Baltic Sedimentary Basin lack dolerite intrusions. The part of the basin in the southern Baltic Sea was subjected to faulting at a different higher degree, as is clear from abundant seismic data collected during extensive offshore oil exploration. A number of faults have been identified in the sedimentary cover (Fig. 11), and most of them formed in the latest Silurian–earliest Devonian times. They were formed by NW–SE compression along the Scandinavian margin of Baltica

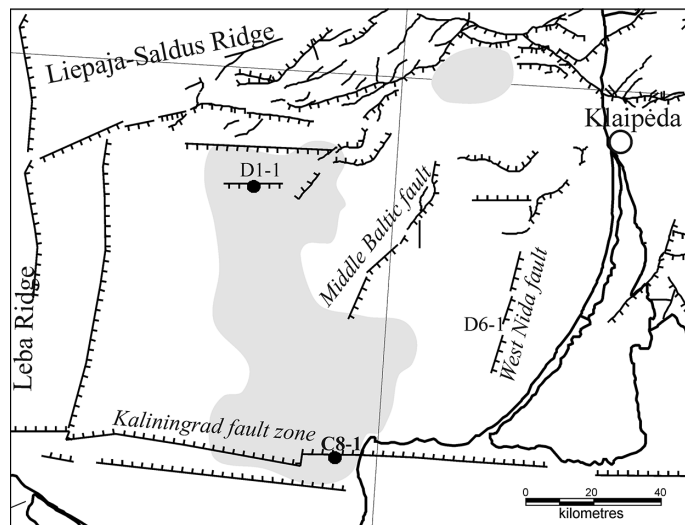


**Fig. 11.** Faults dissecting Palaeozoic sediments. Bold lines show faults (bergstrichs indicate down-thrusted flanks). Wells D1-1 and C8-1 are shown.

during collision with Laurentia in the late Caledonian stage (Šliaupa et al. 2000). Some faults were reactivated in late Devonian (Frasnian–Famennian) and Carboniferous times under a compressional regime (Šliaupa et al. 2004; Poprawa et al. 2006).

The most distinct tectonic feature in the north of the study area is the W–E-oriented fault system bounding the southern margin of the Liepaja–Saldus Ridge. The offsets on the Liepaja–Saldus Ridge border faults reach 500 m. Seismic profiling revealed that some segments were active in the latest Palaeozoic at the latest (Šliaupa & Hoth 2011). The north–south-trending Leba Ridge is the other large-scale tectonic structure. It has a vertical offset of ca 1 km and is bounded by a series of north–south-trending faults that were mostly active in post-Devonian times during late Variscan stages. Some faults can be traced northwards as far as the Gotland area.

The Kaliningrad Fault Zone is a distinct structural feature trending W–E from the Polish offshore to as far as onshore West Lithuania and has a vertical offset of up to 100 m. The age of faulting is not clear due to the absence of late Palaeozoic sediments. It is notable that recent activity of the fault caused the Kaliningrad earthquake of magnitude  $M_L = 5.2$  in 2004 (Gregersen et al. 2007). Dolerite intrusion C8-1 is controlled by the Kaliningrad Fault Zone, but the structural control of dolerite intrusion D1-1 is less clear, although seismic data revealed the presence of a small-amplitude W–E-striking fault in the vicinity (unpublished industrial report).

The alkaline plutonic rocks in northeast Poland reflect a different structural setting. They are located in the crest of the Mazury–Belarus High (Fig. 12) and form a W–E-trending belt that, however, shows no discernible control by large-scale faults. The lack of obvious structural

control is somewhat in conflict with the hypothesis that these intrusions represent the structural continuation of the Pripyat Basin (Demaiffe et al. 2013). Furthermore, the Podlasie–Brest Basin south of the intrusion belt can reasonably be considered as the western continuation of the Dnieper–Donetsk–Pripyat Extension Zone, from which it is separated by the Polesian Saddle (Garetskij et al. 2004). The Polish intrusions are associated with the western part of the Mazury–Belarus High. The total extent of late Palaeozoic uplift exceeded 2 km in northeast Poland as reconstructed from the truncation of sediments overlying the crystalline basement.

In contrast to the magmatic rocks in NE Poland, the Baltic dolerites are situated in the deepest axial part of the Baltic syncline that does not show any evidence for having undergone relative uplift during the Permo-Carboniferous. Instead, the western limit of this igneous area is confined to the large-scale N–S-trending faults bordering the Leba High that was uplifted about 1 km as is clear from truncation of Devonian sediments prior to deposition of Upper Permian sediments.

The earliest Carboniferous igneous activity in the Baltic Sea and NE Poland overlaps in time with the volcanism and plutonism elsewhere in NW Europe. In Great Britain and Ireland, limited rifting north of the Variscan subduction front triggered Tournasian to Viséan-age volcanism of mainly alkaline basic composition (Leeder 1982; Maynard et al. 1997; Timmerman 2004, and references therein). At the same time west of the TTZ in Poland, the deposition of marine clastic sediments prevailed with the formation of carbonate platforms on elevations. Subsidence rates were low and Tournasian and mid-Viséan volcanism of acid to intermediate composition took place in central (Lublin Basin) and northern Poland (Pomerania) northeast of the TTZ during

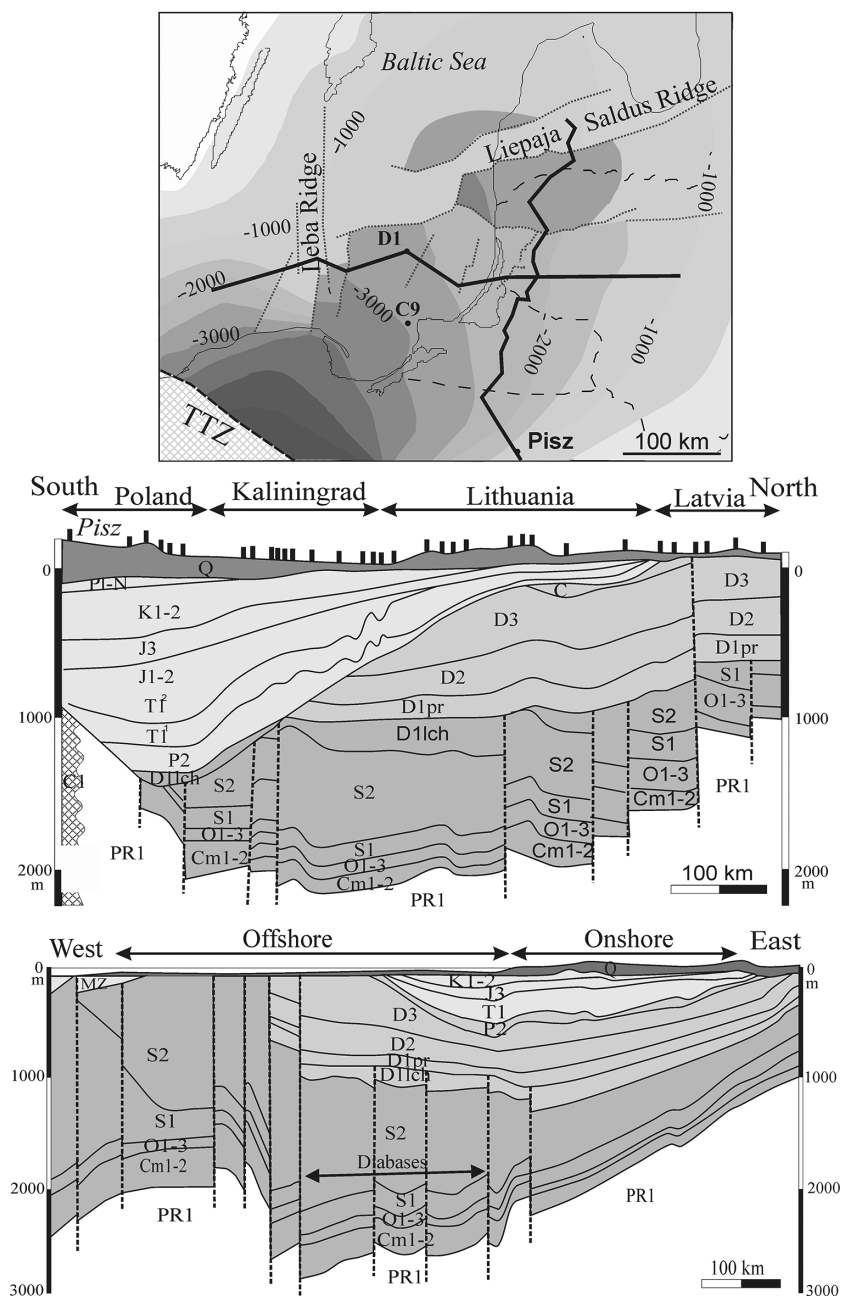


**Fig. 12.** S–N and W–E geological profiles. The upper figure shows locations of profiles and depths of the crystalline basement. Structural complexes are shown in different grey-scale colours.

extension and movement along the TTZ (Narkiewicz 2007). Although the relation between these magmatic provinces and igneous activity in the Baltic Sedimentary Basin area are unclear, the latter might be related alternatively to (i) mantle plume activity or/and (ii) wrenching extension resulting from strike-slip movements along the Tornquist Zone in the west.

The intrusions in northeast Poland and the Baltic Sedimentary Basin may have formed by a mechanism

similar to that of magmatic rocks in the Pripyat rifted basin. The geochemistry and Sr–Nd isotope composition of magmatic rocks, combined with moderate degrees of stretching ( $\beta = 1.1$  to 1.3), suggest that magmatism in the Pripyat–Dnieper–Donetsk Rift was triggered by the upwelling of a thermally and geochemically anomalous mantle plume in late Devonian times (Wilson & Lyashkevich 1996). Furthermore, domal uplift, rifting and magmatism were contemporaneous at several localities

within the eastern East European Craton, suggesting that all these processes have been caused by a cluster of mantle plumes. However, despite the OIB-like composition of the Baltic dolerite, a plume-related origin is unlikely because of the small volumes of magma, the absence of voluminous, rapidly erupted volcanic rocks and the absence of uplift before and during magmatic activity.

Narkiewicz & Narkiewicz (2008) interpret the increasing middle Frasnian to Famennian subsidence rates in the Pripyat and central Lublin basins to have been primarily controlled by intraplate stresses. Similarly, basin formation in Ireland and Britain has been attributed to extension in response to far-field stresses (Coward 1993; Corfield et al. 1996), which also resulted in passive partial melting of the mantle (e.g. Leeder 1982). The likely causes of these events were Carboniferous terrane accretion and collision during the Variscan orogeny in central Europe, which peaked in Viséan times.

However, for the Baltic Sedimentary Basin and northeast Poland there is no evidence for extensive faulting in the Carboniferous that could be linked to magmatism, except for the reactivation of several of the largest fault zones (essentially the Liepaja–Saldus Zone). The Leba Fault Zone post-dates Devonian and pre-dates the deposition of Permian sediments, while the Liepaja–Saldus Zone is a reactivated structure. Faulting took place in a compressional regime as indicated by seismic profiles. Yet, the compressional tectonic phase was most likely initiated after cessation of igneous activity as no cause for far-field tectonic compression can be identified for the Early Carboniferous. The main inversion stage was induced by the propagation of the Variscan Deformation Front and occurred in the Late Carboniferous. For this period, no evidence of lithosphere extension has been reported for the central part of the Baltic Sedimentary Basin either. The parent melts of the dolerite sills probably used pre-existing faults that formed during the Caledonian orogeny.

## CONCLUSIONS

The dolerite sills that intruded Silurian shales in the Baltic Sedimentary Basin are fractionated subalkaline rocks of within-plate affinity, as is also clear from their setting in a continental basin. The parent melts were derived from an enriched mantle source and lack detectable trace element evidence for contamination by crustal material despite having passed through the thick, Palaeoproterozoic continental lithosphere.

The  $351 \pm 11$  Ma  $^{40}\text{Ar}/^{39}\text{Ar}$  plateau age for groundmass plagioclase shows that the sills intruded in the Early Carboniferous and a considerable age gap exists

between the magmatic activity in the Baltic Sea and the 310–250 Ma magmatic rocks in southern Scandinavia and northern Germany. It is clear that the Baltic sills do not form part of this magmatic event and a different tectonic mechanism was responsible for their genesis.

The Baltic dolerites were emplaced coevally with alkaline intrusions in northeast Poland which, however, intruded in a different structural setting. The Baltic sills are confined to the deepest axial part of the Baltic Sedimentary Basin, while the Polish plutons were emplaced in the crest of the Mazury–Belarus High.

The Baltic and NE Poland's alkaline magmatic provinces may be related to the Pripyat Igneous Province, which itself represents the northwestern continuation of the Dnieper–Donetsk Aulacogen. In the latter, igneous activity is related to lithosphere rifting that was perhaps aided by a mantle plume. Considering the small volumes and slow eruption rates, an origin due to the impact of a proper mantle plume is unlikely for the magmatic rocks in the Baltic Sea region and NE Poland.

The magmatic rocks in the Baltic Sedimentary Basin and NE Poland lie in the northwestward prolongation of the Pripyat–Dnieper–Donetsk Rift and may constitute a later phase of magmatic activity in a northwestward propagating rift system. However, no extensional event was recognized in seismic profiles of the Baltic Sea area. Ascending magma must have utilized the pre-existing fault framework. Furthermore, the activity of old faults and formation of scarce new faults took place under a regime of tectonic compression during the Carboniferous and Early Permian, and most likely after the igneous phase. This suggests that some degree of active rifting due to mantle upwelling as the main mechanism driving magmatism in the region cannot be ruled out.

The Permo-Carboniferous magmatic rocks of NW Europe were formed after a considerable (>50–60 Ma) time gap that was characterized by the deposition of platform carbonates and limited rifting. Igneous activity was initiated by wrenching tectonics induced by oblique docking of Gondwana to a collage of recently accreted terranes in western and southern Europe. This mechanism affected the internal parts of the Variscan orogen, its northern foreland and only the westernmost margin of the East European Craton, but no such effects have been recognized in the Baltic Sea region and adjacent areas.

**Acknowledgements.** MJT thanks Jan Wijbrans (Vrije Universiteit, Amsterdam) for the opportunity to date the groundmass plagioclase and Phil Guise for instruction in, and help with, argon mass-spectrometry. The authors thank the reviewer A. Soesoo and an anonymous referee for valuable remarks and corrections.

## REFERENCES

- Aizberg, R. Y., Beskopylny, V. N., Starchik, T. A. & Tsekoyeva, T. K. 2001. Late Devonian magmatism in the Pripyat Palaeorift: a geodynamic model. *Geological Quarterly*, **45**, 349–358.
- Alexander, E. C. Jr., Mickelson, G. M. & Lanphere, M. A. 1978. MMHb-1: a new  $^{40}\text{Ar}$ – $^{39}\text{Ar}$  dating standard. *USGS Open File Report*, **78-701**, 6–8.
- Armbrustmacher, T. J. & Modreski, P. T. 1994. Petrology and mineralogy of alkaline rocks from the Elk massif, north-eastern Poland. *USGS Open-File Report*, **94-145**, 92.
- Breitkreuz, C. & Kennedy, A. 1999. Magmatic flare-up at the Carboniferous/Permian boundary in the NE German Basin revealed by SHRIMP zircon ages. *Tectonophysics*, **266**, 379–404.
- Cabanis, B. & Lecolle, M. 1989. Le diagramme La/10–Y/15–Nb/8 un outil pour la discrimination des séries volcaniques et la mise en évidence des processus de mélange et/ou de contamination crustale. *Comptes Rendus de l'Académie des Sciences, Série II*, **309**, 2023–2029.
- Corfield, S. M., Gawthorpe, R. L., Gage, M., Fraser, A. J. & Besly, B. M. 1996. Inversion tectonics of the Variscan foreland of the British Isles. *Journal of the Geological Society, London*, **153**, 17–32.
- Coward, M. P. 1993. The effect of Late Caledonian and Variscan continental escape tectonics on basement structure, Paleozoic basin kinematics and subsequent Mesozoic basin development in NW Europe. In *Petroleum Geology of Northwest Europe, Proceedings of the 4th Conference* (Parker, J. R., ed.), *The Geological Society, London, Petroleum Geology Conference Series*, **4**, 1095–1108.
- Demaiffe, D., Wiszniewska, J., Krzemińska, E., Williams, I. S., Stein, H., Brassinnes, S., Ohnenstetter, D. & Deloule, E. A. 2013. Hidden alkaline and carbonatite province of Early Carboniferous age in northeast Poland: zircon U–Pb and pyrrhotite Re–Os geochronology. *The Journal of Geology*, **121**, 91–104.
- Dziedzic, A. & Ryka, W. 1983. Carbonatites in the Tajno intrusion (NE Poland). *Archiwum Mineralogiczne*, **38**, 4–34.
- Engels, J. C. & Ingamells, C. O. 1971. *Information Sheets 1 and 2, LP-6 Biotite 40–60 mesh*. U.S.G.S. Menlo Park, California, U.S.A.
- Fitton, J. G., Saunders, A. D., Norry, M. J., Hardarson, B. S. & Taylor, R. N. 1997. Thermal and chemical structure of the Iceland plume. *Earth and Planetary Science Letters*, **153**, 197–208.
- Garetskij, R. G., Aizberg, R. E. & Starchik, T. A. 2004. Pripyatskij trog: tektonika, geodinamika i evolyutsiya [Pripyat Trough: tectonics, geodynamics, and evolution]. *Russian Journal of Earth Sciences*, **6**, 3 [in Russian].
- Gregersen, S., Wiejacz, P., Dębski, W., Domanski, B., Assinovskaya, B. A., Guterch, B., Mäntyniemi, P., Nikulin, V. G., Pacesa, A., Puura, V., Aronov, A. G., Aronova, T. I., Grünthal, G., Husebye, E. S. & Sliupa, S. 2007. The exceptional earthquakes in Kaliningrad district, Russia on September 21, 2004. *Physics of the Earth and Planetary Interiors*, **164**, 1–2, 63–74.
- Heeremans, M., Faleide, J. I. & Larsen, B. T. 2004. Late Carboniferous–Permian of NW Europe: an introduction to a new regional map. In *Permo-Carboniferous Magmatism and Rifting in Europe* (Wilson, M., Neumann, E.-R., Davies, G. R., Timmerman, M. J., Heeremans, M. & Larsen, B. T., eds), *Geological Society, London, Special Publications*, **223**, 75–88.
- Hofmann, A. W., Jochum, K. P., Seufert, M. & White, W. M. 1986. Nb and Pb in oceanic basalts: new constraints on mantle evolution. *Earth and Planetary Science Letters*, **79**, 33–45.
- Kalt, A., Corfu, F. & Wijbrans, J. 2000. Time calibration of a P–T path from a Variscan high-temperature low-pressure metamorphic complex (Bayerische Wald, Germany), and the detection of inherited monazite. *Contributions to Mineralogy and Petrology*, **138**, 143–163.
- Kharin, G. S. & Eroshenko, D. V. 2014. Basic intrusives and hydrocarbonic potential of the South-East Baltic. *Oceanology*, **54**, 245–258.
- Koppers, A. A. P. 2002. ArArCALC – Software for  $^{40}\text{Ar}/^{39}\text{Ar}$  age calculations. *Computers & Geosciences*, **28**, 605–619.
- Korzun, V. P. & Makhnach, A. S. 1977. *Verkhnedevonskaya shchelochnaya vulkanogennaya formatsiya Pripyatskoj vpadiny* [Upper Devonian Alkaline Volcanogenic Formation of the Pripiat Trough]. Nauka i tekhnika, Minsk, 160 pp. [in Russian].
- Kruchek, S. A. & Obukhovskaya, T. G. 1997. Detal'naya stratigrafiya devonskikh otlozhenij Zhlobinskoj sedloviny i sopredel'nykh regionov v kontekste poiskov mineral'nykh resursov [Detailed stratigraphy of Devonian deposits of the Zhlobin Saddle and adjoining regions in the context of searching for mineral resources]. In *Mineral'no-syrevaya baza Respubliki Belarus: sostoyanie i perspektivy* [Mineral Resources of the Republic of Belarus: State of the Art and Outlooks], pp. 19–21. BelNIGRI, Minsk [in Russian].
- Krystkiewicz, E. & Krzemiński, L. 1992. Petrology of the alkaline ultrabasic Tajno complex. *Prace Panstwowego Instytutu Geologicznego*, **139**, 19–35.
- Krzemińska, E. & Krzemiński, L. 2012. The Mława syenite alkaline intrusion – A perspective of rare earth elements occurrence. *Buletyn Panstwowego Instytutu Geologicznego*, **448**, 401–408.
- Krzemińska, E., Wiszniewska, J. & Williams, I. S. 2006. Early Carboniferous age of the cratonic intrusions in the crystalline basement of NE Poland. *Przegląd Geologiczny*, **54**, 1093–1098.
- Kuszniur, N. J., Kovkhuto, A. & Stephenson, R. A. 1996. Syn-rift evolution of the Pripyat Trough: constraints from structural and stratigraphic modelling. *Tectonophysics*, **268**, 221–236.
- Leeder, M. 1982. Upper Palaeozoic basins of the British Isles – Caledonide inheritance versus Hercynian plate margin processes. *Journal of the Geological Society of London*, **139**, 479–491.
- Ludwig, K. R. 1998. *Using Isoplot/Excel Version 1.00. A Geochronological Toolkit for Microsoft Excel*. Berkeley Geochronology Center Special Publication No. 1, 44 pp.
- Maynard, J. R., Hofmann, W., Dunay, R. E., Bentham, P. N., Dean, K. P. & Watson, I. 1997. The Carboniferous of Western Europe: the development of a petroleum system. *Petroleum Geoscience*, **3**, 97–115.
- McDonough, W. F., Sun, S. S., Ringwood, A. E., Jagoutz, E. & Hofmann, A. W. 1992. K, Rb and Cs in the Earth and Moon and the evolution of the Earth's mantle. *Geochimica et Cosmochimica Acta*, **56**, 1001–1012.

- Meschede, M. 1986. A method of discriminating between different types of mid-ocean basalts and continental tholeiites with the Nb–Zr–Y diagram. *Chemical Geology*, **56**, 207–218.
- Mikhailov, N. D., Laptsevich, A. G. & Vladykin, N. V. 2010. Izotopnyj sostav Sr i Nd v verkhnedevonskikh magmaticheskikh porodakh Belorusi [Sr and Nd isotopic composition of the Upper Devonian igneous rocks of Belarus]. *Doklady Natsional'noj Akademii Nauk Belorusi*, **54**, 6, 100–104.
- Motuza, G., Kepežinskas, P. & Šliaupa, S. 1994. Diabases from drillhole D-1 in the Baltic Sea. *Geologija (Vilnius)*, **16**, 16–20.
- Narkiewicz, M. 2007. Development and inversion of Devonian and Carboniferous basins in the eastern part of the Variscan foreland (Poland). *Geological Quarterly*, **51**, 231–256.
- Narkiewicz, K. & Narkiewicz, M. 2008. The mid-Frasnian subsidence pulse in the Lublin Basin (SE Poland): sedimentary record, conodont biostratigraphy and regional significance. *Acta Geologica Polonica*, **58**, 287–301.
- Neumann, E.-R., Wilson, M., Heeremans, M., Spencer, E. A., Obst, K., Timmerman, M. J. & Kirstein, L. 2004. Carboniferous–Permian rifting and magmatism in southern Scandinavia, the North Sea and northern Germany: a review. In *Permo-Carboniferous Rifting and Magmatism in Europe* (Wilson, M., Neumann, E.-R., Davies, G. R., Timmerman, M. J., Heeremans, M. & Larsen, B. T., eds), *Geological Society of London, Special Publications*, **223**, 11–40.
- Pearce, J. A. 1983. The role of subcontinental lithosphere in magma genesis at destructive plate margins. In *Continental Basalts and Mantle Xenoliths* (Hawthorn, C. J. & Norry, M. J., eds), pp. 230–249. Nantwich, Shiva.
- Pearce, J. A. 1996. A user's guide to basalt discrimination diagrams. In *Trace Element Geochemistry of Volcanic Rocks; Applications for Massive Sulphide Exploration* (Bailes, A. H., Christiansen, E. H., Galley, A. G., Jenner, G. A., Keith, J. D., Kerrich, R., Lentz, D. R., Leshner, C. M., Lucas, S. B., Ludden, J. N. et al., eds), *Geological Association of Canada, Short Course Notes*, **12**, 79–113.
- Petrova, N. S., Shablovskaya, R. K. & Krasnik, Z. M. 1983. O khimiko-mineralogicheskom sostave tufogennykh glinistykh prosloev nadsolveykh i solenosnykh otlozhenij Pripyatskogo progiba [Chemical and mineralogical composition of tufogenic argillaceous layers of evaporitic and covering deposits of the Pripyat Trough]. *Doklady Natsional'noj Akademii Nauk Belorusi*, **27**, 835–837 [in Russian].
- Poprawa, P., Šliaupa, S. & Sidorov, V. 2006. Późnosylursko-wczesnodewońska śródplytowa kompresja na przedpolu orogenu kaledońskiego (centralna część basenu bałtyckiego) – analiza danych sejsmicznych [Late Silurian–Early Devonian intra-plate compression in the foreland of the Caledonian orogen (central part of the Baltic Basin) – analysis of seismic data]. *Prace Państwowego Instytutu Geologicznego*, **186**, 215–224 [in Polish].
- Renne, P. R., Swisher, C. C., Deino, A. L., Karner, D. B., Owens, T. L. & DePaolo, D. J. 1997. Intercalibration of standards, absolute ages and uncertainties in  $^{40}\text{Ar}/^{39}\text{Ar}$  dating. *Chemical Geology*, **145**, 117–152. See also Corrigendum in *Chemical Geology*, **149**, p. 259.
- Rex, D. C. & Guise, P. G. 1986. Age of the Tinto felsite, Lanarkshire: a possible  $^{39}\text{Ar}$ – $^{40}\text{Ar}$  monitor. *Bulletin of Liaison and Information, IGCP Project 196*, 6.
- Rex, D. C., Guise, P. G. & Wartho, J.-A. 1993. Disturbed  $^{40}\text{Ar}$ – $^{39}\text{Ar}$  spectra from hornblendes: thermal loss or contamination? *Chemical Geology (Isotope Geoscience Section)*, **103**, 271–281.
- Roddick, J. C. 1983. High precision intercalibration of  $^{40}\text{Ar}$ – $^{39}\text{Ar}$  standards. *Geochimica et Cosmochimica Acta*, **47**, 887–898.
- Ryka, W. 1992. Geology of the Tajno massif carbonatites. *Prace Państwowego Instytutu Geologicznego*, **CXXXIX**, 43–77.
- Ryka, W., Armbrustmacher, T. J. & Modreski, P. J. 1992. Geochemistry and petrology of the alkaline rocks of the Tajno complex (Preliminary report). *Prace Państwowego Instytutu Geologicznego*, **CXXXIX**, 37–41.
- Šliaupa, S. & Hoth, P. 2011. Geological evolution and resources of the Baltic Sea area from the Precambrian to the Quaternary. In *The Baltic Sea Basin* (Harff, J., Björck, S. & Hoth, P., eds), pp. 13–51. Springer, Berlin.
- Šliaupa, S., Motuza, G., Timermann, M. & Korabliova, L. 2002. Age and distribution of the diabase intrusions of the Baltic Sea. In *7th Marine Geological Conference "Baltic-7" Abstracts, Kaliningrad*, p. 122.
- Šliaupa, S., Poprawa, P. & Jacyna, J. 2000. Structural analysis of seismic data in the Baltic Basin: evidences for Silurian–Early Devonian intra-plate compression in the foreland of Caledonian orogen. *Journal of Czech Geological Society*, **45**, 260–261.
- Šliaupa, S., Laskova, L., Lazauskiene, J., Laskovas, J. & Sidorov, V. 2004. The petroleum system of the Lithuanian offshore region. *Zeitschrift für Angewandte Geologie*, **2**, 41–62.
- Steiger, R. H. & Jäger, E. 1977. Subcommission on geochronology: convention on the use of decay constants in geo- and cosmochronology. *Earth and Planetary Science Letters*, **36**, 359–362.
- Sun, S. S. & McDonough, W. F. 1989. Chemical and isotopic systematic of oceanic basalts: implication for mantle composition and processes. In *Magmatism in the Ocean Basins* (Saunders, A. D. & Norry, M. J., eds), *Geological Society, London, Special Publications*, **42**, 313–345.
- Timmerman, M. J. 2004. Timing, geodynamic setting and character of Permo-Carboniferous magmatism in the foreland of the Variscan Orogen, NW Europe. In *Permo-Carboniferous Magmatism and Rifting in Europe* (Wilson, M., Neumann, E.-R., Davies, G. R., Timmerman, M. J., Heeremans, M. & Larsen, B. T., eds), *Geological Society, London, Special Publications*, **223**, 41–74.
- Timmerman, M. J., Heeremans, M., Kirstein, L. A., Larsen, B. T., Spencer-Dunworth, E. A. & Sundvoll, B. 2009. Linking changes in tectonic style with magmatism in northern Europe during the late Carboniferous to latest Permian. *Tectonophysics*, **473**, 375–390.
- Turner, G., Huneke, J. C., Podosek, F. A. & Wasserburg, G. J. 1971.  $^{40}\text{Ar}$ – $^{39}\text{Ar}$  ages and cosmic ray exposure ages of Apollo 14 samples. *Earth and Planetary Science Letters*, **12**, 19–35.
- Vejelyte, I., Yi, K., Cho, M., Kim, N. & Lee, T. 2011. Intracratonic carboniferous granites in the Paleoproterozoic crust of Lithuania: new SHRIMP U–Pb zircon ages. In *Goldschmidt Conference Abstracts*, p. 2079.

- Veretennikov, N. V., Korzun, V. P., Korneichik, A. V., Mikhailov, N. D., Laptsevich, A. G. & Shkuratov, B. I. 1997. Diatremy Belarusi (petrologicheskaya spetsializatsiya, almazonosnost') [Belorussian diatremes (petrological specialization, diamond potential)]. In *Mineral'no-syrevaya baza Respubliki Belarus: sostoyanie i perspektivy* [*Mineral Resources of the Republic of Belarus: State of the Art and Outlooks*], pp. 101–102. BelNIGRI, Minsk [in Russian].
- Wijbrans, J. R., Pringle, M. S., Koppers, A. A. P. & Scheveers, R. 1995. Argon geochronology of small samples using the Vulkan argon laserprobe. *Proceedings of the Koninklijke Nederlandse Akademie van Wetenschappen*, **98**, 185–218.
- Wilson, M. & Lyashkevich, Z. M. 1996. Magmatism and the geodynamics of rifting of the Pripyat-Dnieper-Donets Rift, East European Platform. *Tectonophysics*, **268**, 65–81.
- Winchester, J. A. & Floyd, P. A. 1977. Geochemical discrimination of different magma series and their differentiation products using immobile elements. *Chemical Geology*, **20**, 325–343.
- Wood, D. A. 1980. The application of Th–Hf–Ta diagram to problems of tectonomagmatic classification and to establishing the nature of crustal contamination of basaltic lavas of the British Tertiary Volcanic Province. *Earth and Planetary Science Letters*, **50**, 11–30.

## Läänemere lõunaosa Vara-Karboni doleriitsete sillide geokeemia ja $^{40}\text{Ar}/^{39}\text{Ar}$ isotoopvanus

Gediminas Motuza, Saulius Šliaupa ja Martin J. Timmerman

Vara-Karboni doleriitised intrusioonid on teada Läänemere lõunaosas, arvatavasti 30–60 km laiusel lääne-ida-suunalisel ja 100 km pikkusel põhja-lõunasuunalisel alal. Puuraugust D1-1 võetud doleriidiproovide koostist uuriti keemiliselt ja vanus määrati  $^{40}\text{Ar}/^{39}\text{Ar}$  astmelise kuumutamise meetodil. Kontinentaalse riftistumise tingimustes vahevööst pärit magmast tekkinud doleriidid on leelise- ja naatriumirikkad kivimid, mida iseloomustab suur  $\text{TiO}_2$  (3,92 ja 3,99 wt%),  $\text{P}_2\text{O}_5$  (1,67 ja 1,77 wt%) ning kergete muldmetallide sisaldus. Põhimassi plagioklasside  $^{40}\text{Ar}/^{39}\text{Ar}$  platoovanus on  $351 \pm 11$  Ma. Magmakivimite puudumine ajavahemikul 310–250 Ma Lõuna-Skandinaavias ja Põhja-Saksamaal viitab vähesele magmalisele tegevusele sel perioodil. Läänemere lõunaosa sillid on Kirde-Poolas teadaolevate leeliskivimite intrusioonidega samavanused. Eelmainitud alad moodustavad Prõpjatsi-Dnepri-Donetski rifti-süsteemi (370–359 Ma) loodesuunalise jätku ja võisid seotud olla rifti arengu hiliseima faasiga.